Modeling of Tunneling Effects in Epsilon-Near-Zero Waveguide

Nebojša Vojnović[1], Miranda Mitrović[1] and Branka Jokanović[1]

Abstract – **In this paper we present a simple method for efficient modeling of the tunneling effect in a non-homogeneous epsilon-near-zero (ENZ) waveguide, using an equivalent circuit approach. ENZ waveguide consists of rectangular waveguides filled with two-layered dielectric, E-step, and a narrow channel. It was shown that the E-step in a non-homogenous structure can be modeled rather simply using a shunt capacitor whose capacitance is determined analytically using the same expression which applies to homogeneous rectangular waveguide. In that case the error in determining the first resonance is less than 1%, while in the case of the second resonance the error is less than 2.5%, if the non-homogeneity is not very large, i.e. if the ratio between the relative permittivities of the dielectrics in the input waveguides and the channel is less than two.**

Keywords – **ENZ waveguide, E-step discontinuity, Tunneling effect, Equivalent circuit**

I. INTRODUCTION

In the last couple of years, since it was theoretically shown that energy transfer through very narrowed waveguide structures consisting of input waveguides and a channel between them is possible [1], a large number of papers considering this phenomenon and it's applications was published. This phenomenon puts waveguide transmission systems in an entirely new context, giving them a series of new applications. The transfer of energy through these systems, or so called "tunneling", occurs just below the cut-off frequency of the fundamental mode in the narrow channel, if the channel is formed only by changing the input rectangular waveguide height. At the tunneling frequency, dielectric in the channel has an effective permittivity close to zero and is thus called epsilon-near-zero, or ENZ channel. Also, at the tunneling frequency, wavelength becomes infinitely large and the phase shift becomes zero, so the tunneling frequency is also known as the zero-order, or ZOR resonance. Tunneling effect can be achieved even above the cut-off frequency of the fundamental mode by reducing the width of the channel. In a narrowed ENZ channel, the dielectric permittivity can be greater than dielectric permittivity in the input waveguides, which is not the case with a classical design.

ENZ waveguides are multi-band structures since besides the tunneling effect, so called Fabry-Perot resonances also occur. These Fabry-Perot resonances strongly depend on the length of the channel, which is not the case with the ZOR resonance. ZOR resonance is determined by the width of the channel and relative permittivity of the dielectric in the channel. Tunneling effect has been experimentally verified at microwave frequencies using rectangular waveguide dispersion characteristics near the cut-off frequency of TE_{10} mode [2]. It was shown that a similar effect could be achieved by using complementary split-ring resonators mounted on the surface of the channel [3], and also by using thin wire grid placed along the channel, in which the tunneling frequency no longer depends on the dielectric constant in the channel, but on the diameter of the wire conductors. As a result, the possibility of multi-band operation is demonstrated in [4] using two separate channels of the same dielectric constant. A variant of ENZ waveguide which is very convenient for implementation, as it allows control over the attenuation in the channel, is the use of a microwave substrate which serves as both the ENZ channel, and as a support for the input waveguides proposed in [5]. Microwave substrates are strictly defined in terms of thickness of the dielectric and metallization roughness, both of which strongly influence the attenuation in the channel, as it has been shown in [6].

The possibility of shifting the resonant frequency of ENZ structures has been demonstrated so far only in two papers: in [7], where the ZOR shift has been performed using a varactor diode, and in [5], by changing the length of two slots on the channel surface.

In addition to the increase of the possibilities of today's computers, and thus their ability to solve larger and more complex problems in the field of electromagnetics, the importance of presenting a problem using equivalent circuits does not lose on its importance. The purpose of using equivalent circuits is a significant save of time and memory resources, compared to using a full-wave electromagnetic solver, with a sufficient accuracy. The accuracy of the obtained results largely depends on the fidelity with which the equivalent circuit approximates the real physics behind the problem. It is possible to find equivalent circuits [8], [9] which model complex problems very precisely, even at high frequencies.

The role of the equivalent circuit is more noticable in optimization process since it allows much faster optimization in respect to time consuming full-wave simulations with high demands regarding computer resources.

The aim of this paper is to show the accuracy of modeling ENZ waveguide structures using an equivalent circuit, with respect to the non-homogeneity of the input waveguides consisting of a two-layer dielectric: a thin dielectric layer, which is an extension of the ENZ channel, and a thick dielectric which fills the rest of the input waveguide. It should be noted that there is not an equivalent circuit model for E-

[1] The authors are with the Institute of Physics, University of Belgrade, Pregrevica 118, 11080 Beograd, Serbia, E-mail: nebojsav@ipb.ac.rs.

step discontinuity of this kind of structure to be found in the literature. To model this discontinuity we will use a model valid for the E-step discontinuity in a waveguide with homogeneous dielectric, but with a minor modification which takes into account the existence of a two-layer dielectric in the input waveguide.

II. NOVEL ENZ WAVEGUIDE DESIGN

In this paper, the ENZ waveguide structure proposed in [6] is modeled, in which a channel extends along the input waveguides so that the input waveguides consist of two different substrates. The non-homogeneous structure of the input waveguides is depicted in Fig. 1. Dielectrics in the input waveguides and channel are marked with different colors, and the whole structure has a metal coating, except for the leftmost and the rightmost side where the waveguide ports are placed. The following dimensions were used:

- a – width of the input waveguide
- b – height of the input waveguide
- L_w – lenght of the input waveguide
- b_{ch} – channel height
- L_{ch} – channel lenght
- ε_{rw} – relative permittivity of the upper dielectric in the input waveguide
- ε_{rch} – relative permittivity in the channel.

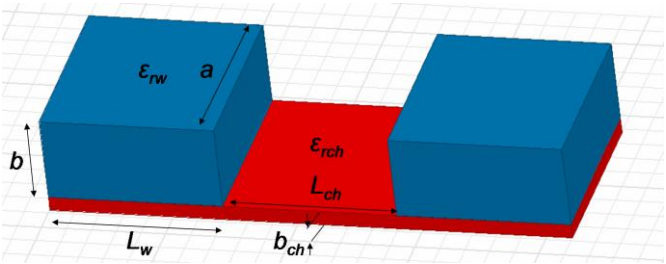

Fig. 1. ENZ waveguide with relevant dimensions: a=7.62mm, b=4.06mm, b_{ch}=0.254mm, L_w=7mm, L_{ch}=7mm, ε_{rw}=5.95 and ε_{rch}=3

To support tunneling, ENZ waveguide must have two E-step discontinuities as was shown in [5]. If the structure consists only of the input waveguide and the channel, the tunneling effect does not occur.

As the Fig. 1 shows, the input waveguides consist of two dielectrics, which further complicates the approximation of this part of the structure with the equivalent circuit. Relative permittivity condition which must be met in order to have tunneling can be found in literature [2]:

$$\frac{\varepsilon_{rw}}{4} \le \varepsilon_{rch} \le \varepsilon_{rw}. \qquad (1)$$

However, even if this condition is not met, tunneling in the structure may occur if the channel width is sufficiently reduced.

Fig. 2 gives a typical frequency dependence of reflection and transmission coefficients for this structure, obtained by full-wave 3D simulation for two different channel and input waveguide height ratios. In this picture two resonant frequencies marked with ZOR (zero-order resonance - tunneling frequency) and FP (Fabry-Perot) resonance are clearly visible. It will be shown that the tunneling frequency is not sensitive to the changes in the length of the channel, which is not the case with the FP resonance.

In addition, mechanisms behind these resonances are not the same, which can be seen from Fig. 3 and Fig. 4, which show the field distribution along the channel for both cases. In Fig. 3 it can be seen that the tunneling frequency exhibits no phase shift along the channel. On the other hand, Fig. 4 clearly shows a standing wave formed in the channel with the maximums at the open ends of the channel.

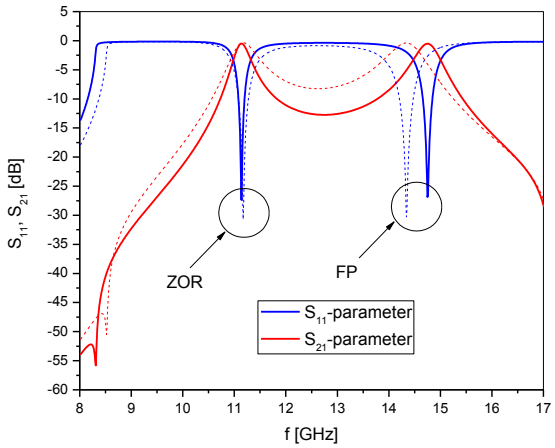

Fig. 2. Simulated S-parameters for ENZ waveguide in Fig. 1 for different b_{ch}/b ratios: b_{ch}/b=0.06 (solid line), b_{ch}/b=0.12 (dashed line)

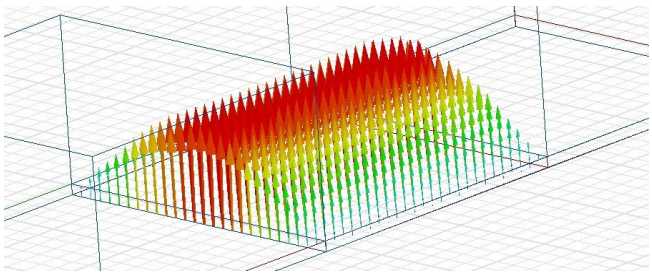

Fig. 3. Electric field distribution in the channel at the tunneling frequency

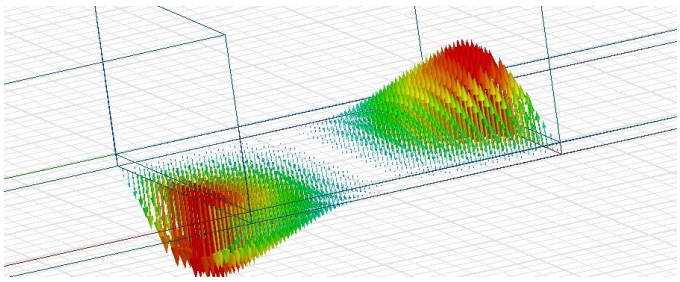

Fig. 4. Electric field distribution in the channel at FP resonance

III. THE EQUIVALENT CIRCUIT

Fig. 5 depicts an ENZ waveguide equivalent circuit in which the input waveguides and the channel are modeled using transmission line sections with Z^c_w, β_w and L_w, and Z^c_{ch}, β_{ch} and L_{ch} parameters, respectively. It should be noted that Z^c_w and Z^c_{ch} are characteristic impedances of the equivalent transmission lines, and not wave impedances of TE waves in the waveguides. E-step is modeled using a capacitor C.

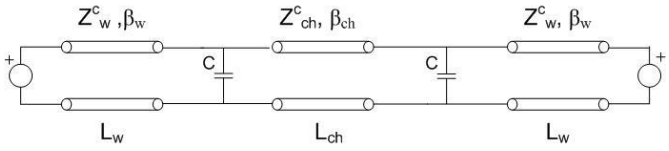

Fig. 5. Equivalent circuit for the structure in Fig. 1

We emphasize that there is another way to model the waveguide change in height by using capacitors and ideal transformers [10]. However, the equivalent circuit in Fig. 5 is simpler, and gives the results of the same accuracy.

As it was previously mentioned in the introduction, there are two dielectric slabs placed perpendicular to the electric field vector in the input waveguides. Therefore, instead of the classical formulation of the phase coefficient for the TE wave, an expression for the guided wavelength in this kind of structure was taken from the literature [11]:

$$\lambda_{gw} = \frac{\lambda_0}{\sqrt{\dfrac{\varepsilon_{rch}}{1-\dfrac{b-b_{ch}}{b}\left(1-\dfrac{\varepsilon_{rch}}{\varepsilon_{rw}}\right)} - \left(\dfrac{\lambda_0}{2a}\right)^2}}. \tag{2}$$

Here, λ_0 stands for the free-space wavelength. The phase coefficient and wave impedance in input waveguides, β_w and Z^w_w, are given by the following expressions:

$$\beta_w = \frac{2\pi}{\lambda_{gw}} \tag{3}$$

$$Z^w_w = \frac{\omega\mu_0}{\beta_w}. \tag{4}$$

Using of the classical relation for calculating the phase coefficients in the input waveguides for TE waves would require some kind of dielectric homogenization, which was avoided by implementing (2). By comparing the calculated and simulated values for the guided wavelength in the input waveguide, a perfect agreement was observed, regardless of the dielectric constant, and thus confirming the validity of the expression (2).

Unlike the input waveguides, the channel consists of only one dielectric, and it is possible to use the classic formulation for the TE waves. The parameters of the channel, i.e. the phase coefficient β_{ch}, and the wave impedance of the TE_{10} wave Z^w_{ch}, are given by:

$$\beta_{ch} = \sqrt{\omega^2\mu_0\varepsilon_0\varepsilon_{rch} - \left(\frac{\pi}{a}\right)^2} \tag{5}$$

$$Z^w_{ch} = \frac{\omega\mu_0}{\beta_{ch}}. \tag{6}$$

It is necessary to get the characteristic impedances which describe the transmission line sections from the TE_{10} wave impedances. The waveguide wave impedance is defined as the ratio between the electric and magnetic field intensities, and the characteristic impedance of the equivalent transmission line is given as the ratio between the voltage and the current in a given point of the transmission line. Bearing in mind that the voltage and current are defined as line integrals of the electric and magnetic field, respectively, it becomes clear that it is possible to approximate the characteristic impedances of the transmission lines with the expressions of the form:

$$Z^c_w = \frac{2b}{a} Z^w_w \tag{7}$$

$$Z^c_{ch} = \frac{2b_{ch}}{a} Z^w_{ch}. \tag{8}$$

Factor 2 in relations (7) and (8) is placed to compensate the sinus distribution of the electric field along the width of a rectangular waveguide.

Special attention must be paid to the modeling of the waveguide with the TE_{10} wave, if the operating frequency is below the cut-off frequency of the dominant mode. For the case when the operating frequency is above the cut-off frequency of the TE_{10} mode, there is wave propagation in the waveguide and the expression under the square root in (5) is positive. It should be noted that the square root in the expression (5) is a real mathematical operation.

However, when the operating frequency is below the cut-off frequency of the TE_{10} mode, evanescent waves with strongly pronounced attenuation are present in the waveguide, and instead of equation (5) we should use an expression of the form:

$$\gamma_{ch} = j\sqrt{\omega^2\mu_0\varepsilon_0\varepsilon_{rch} - \left(\frac{\pi}{a}\right)^2}, \tag{9}$$

where γ_{ch} marks the complex propagation coefficient in the channel. In equation (9) the square root is a complex mathematical operation and it can provide a solution with either a positive or a negative sign. This prefix should be chosen so that the real part of the complex propagation coefficient in the channel, $Re\{\gamma_{ch}\}$, is greater than zero, which corresponds to the nature of the evanescent waves. Lossless equivalent transmission lines were used for modeling of the waveguide sections.

Waveguide height changes were modeled using shunt capacitors. This was done in order to adequately model the surplus charge that accumulates on the vertical walls in places where the change of height occurs. The expressions used to define the capacitances of these capacitors were taken from [11] for the case of asymmetric coupling of two waveguides. Based on these expressions, frequency dependence of this capacitance for several different types of dielectric in the channel was derived, as shown in Fig. 6. It should be noted that the expression for the capacitance was derived for the case when the dielectrics in both waveguides are identical, and strictly speaking does not match the case when the input waveguide is filled with two-layered dielectric as in Fig. 1.

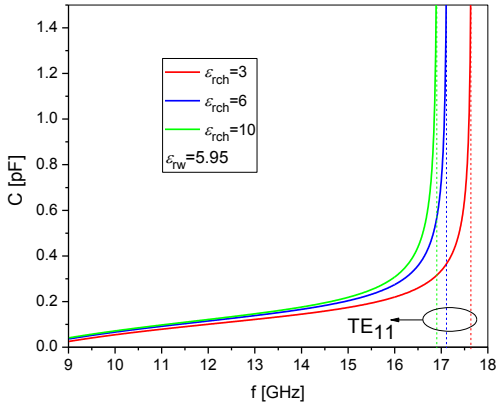

Fig. 6 Frequency dependance of the shunt capacitance for several different dielectrics in the channel

Fig. 6 shows that this capacitance has a singularity which occurs when the condition $b=\lambda_{gw}/2$ is met, which happens at the cut-off frequency of the next mode that involves the change of the electric field along the waveguide height, i.e. at the cut-off frequency of the TE_{11} mode in the input waveguides. The error of the expressions defining the capacitance can be lower than 1% if a condition $2b/\lambda_{gw}\leq 1$ is fulfilled. It is worth mentioning that the capacitance illustrated in Fig. 6 is singular in the sense that at the frequency f_{cTE11} it will have infinitely large value and therefore at that frequency in the circuit from Fig. 5, a short-circuit can be placed instead of the capacitors.

All sections in Fig. 5 were modeled using the appropriate ABCD matrices, whose parameters for each element in the circuit were taken from [12]. After cascading these ABCD matrices and their multiplication, the obtained ABCD parameters were transformed into the scattering parameters (*S*-parameters) using the relations given in [12].

IV. COMPARING THE SIMULATION RESULTS

In this section an overview of the ENZ waveguide simulated S-parameters obtained using the equivalent model and full-wave analysis, will be presented.

To demonstrate the results, an ENZ waveguide with the following input waveguide dimensions was chosen: width a=7.62mm, height b=4.06mm and length L_w=7mm, while the channel's height is b_{ch}=0.254mm and length L_{ch}=7mm. Relative permittivities of the input waveguide and the channel are ε_{rw}=5.95 and ε_{rch}=3, respectively.

The transmission coefficient, S_{21}, in the considered structure for three different values of channel length is shown in Fig. 7. The figure shows that the change in length of the channel can affect the position of the FP resonance to a much greater extent, while the change in position of the ZOR is rather small. In other words, ZOR practically does not depend on the length of the channel, while the FP resonance does.

For the case of the channel length equal to 7mm, equivalent model is making an error in estimating the position of the ZOR and FP resonances of 0.7% and 0.9%, respectively. As for the case when the channel length is equal to 10mm, the errors are 0.5% and 0.1%, respectively. If the channel is 14mm long, the error in predicting the positions of ZOR and FP resonances are 0.4% and 0.8%, respectively.

Therefore, it can be concluded that the results obtained using equivalent circuit model are in a very good agreement with the results obtained from the full-wave simulation, since the difference between the two ways of calculating the resonances is less than 1% for both of the resonant frequencies.

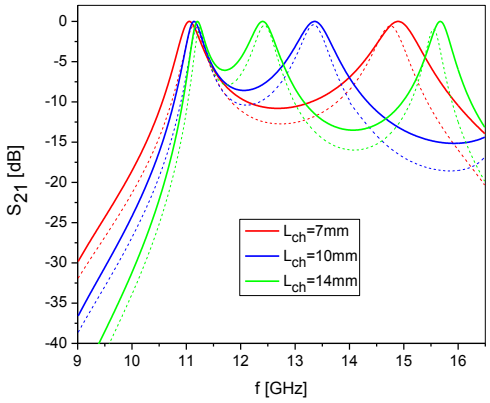

Fig. 7. Transmission coefficient, $S_{21,}$ for equivalent (solid line) and full-wave model (dashed line) for three different channel lengths: L_{ch}=7, 10, 14mm

Fig. 8 shows the transmission coefficient in the considered structure for three different values of the relative permittivity of the dielectric filling the channel. For the case when the channel dielectric has relative permittivity ε_{rch}=2, the errors in the positions of ZOR and FP resonances are 1.5% and 2.5%, respectively. If the relative permittivity of the channel is chosen to be ε_{rch}=4, the errors are 0.4% and 1.4%, respectively. The same figure shows the case when the channel relative permittivity is ε_{rch}=3, as a referent case.

It can be concluded that the equivalent model makes a smaller error if the relative permittivity of the channel increases, compared to the case when ε_{rch} decreases, which makes sense because increasing the dielectric constant of the channel reduces the discontinuity between the dielectrics in the input waveguide. In both cases, the error does not exceed 2.5%, and it can be said that the agreement between the results obtained using the equivalent circuit and 3D simulation is very good. It should be noted that when changing the relative permittivity of the channel, the condition (1) must always be satisfied.

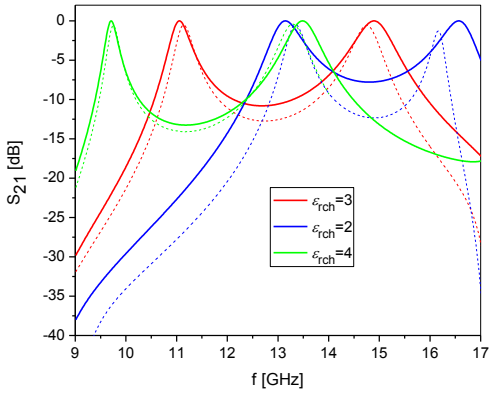

Fig. 8. Transmission coefficient, $S_{21,}$ obtained using the equivalent circuit (solid line) and full-wave analysis (dashed line) for three different dielectrics in the channel (ε_{rw}=5.95)

V. TUNNELING FREQUENCY CALCULATION

Now we will address the conditions that must be met in order to have a resonance in this structure. In [5], a tunneling condition at the ZOR frequency was derived:

$$f_{tun} = \frac{c}{2a\sqrt{\varepsilon_{rch}}}, \tag{10}$$

which means that the tunneling effect occurs precisely at the cut-off frequency of the dominant mode in the channel.

According to the markings from Fig. 9 following expressions can be written:

$$Z_1 = Z^c{}_w, \tag{11}$$

$$Z_2 = Z_1 \square \frac{1}{j\omega C}, \tag{12}$$

$$Z_3 = Z^c{}_{ch}\frac{Z_2 + jZ^c{}_{ch}\tan(\beta_{ch}L_{ch})}{Z^c{}_{ch} + jZ_2\tan(\beta_{ch}L_{ch})}, \tag{13}$$

$$Z_4 = Z_3 \square \frac{1}{j\omega C}, \tag{14}$$

$$Z_{in} = Z^c{}_w\frac{Z_4 + jZ^c{}_w\tan(\beta_w L_w)}{Z^c{}_w + jZ_4\tan(\beta_w L_w)}. \tag{15}$$

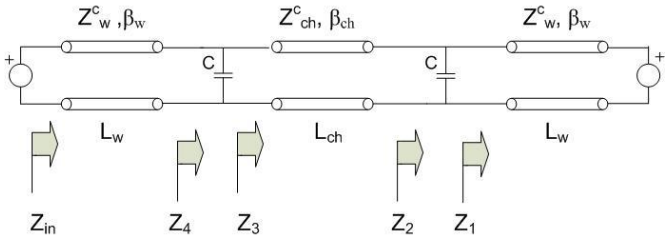

Fig. 9. - Equivalent circuit of the considered structure with all the relevant markings

The condition that needs to be fulfilled in order to have a resonance, is to have a perfect match at the input of the structure, i.e. $Z_{in}=Z^c{}_w$.

After solving the equations (11)-(15), two transcedental relations are obtained:

$$\begin{aligned}&\left[Z^c{}_{ch}{}^3X_{cond}{}^2 + Z^c{}_w{}^2Z^c{}_{ch}{}^3 - Z^c{}_w{}^2Z^c{}_{ch}X_{cond}{}^2\right]\tan(b_{ch}L_{ch})^2 + \\ &+\left[Z^c{}_{ch}{}^2X_{cond}{}^3 + 3Z^c{}_w{}^2Z^c{}_{ch}{}^2X_{cond} - Z^c{}_w{}^2X_{cond}{}^3\right]\tan(b_{ch}L_{ch}) + \\ &+2Z^c{}_w{}^2Z^c{}_{ch}X_{cond}{}^2 = 0,\end{aligned} \tag{16}$$

$$\begin{aligned}&[Z^c{}_{ch}{}^2X_{cond}{}^4 - Z^c{}_w{}^2X_{cond}{}^4 - Z^c{}_{ch}{}^4X_{cond}{}^2 + \\ &+2Z^c{}_w{}^2Z^c{}_{ch}{}^2X_{cond}{}^2 - Z^c{}_w{}^2Z^c{}_{ch}{}^4]\tan(\beta_{ch}L_{ch})^2 \\ &+\left[4Z^c{}_w{}^2Z^c{}_{ch}X_{cond}{}^3 - 2Z^c{}_{ch}{}^3X_{cond}{}^3 - 4Z^c{}_w{}^2Z^c{}_{ch}{}^3X_{cond}\right]\tan(\beta_{ch}L_{ch}) - \\ &-4Z^c{}_w{}^2Z^c{}_{ch}{}^2X_{cond}{}^2 = 0,\end{aligned} \tag{17}$$

where $X_{cond} = -1/\omega C$.

The condition (16) forms a discrete set of frequency points at which the imaginary part of the impedance Z_{in} is equal to zero. Similarly, the condition (17) forms a discrete set of frequency points at which the real part of the impedance Z_{in} is equal to $Z^c{}_w$. The intersection of these two sets of frequency points provides a set of tunneling frequencies for the considered structure, i.e. a set of frequencies for which the tunneling condition is fulfilled.

Fig. 10 shows the real and imaginary parts of the impedance Z_4 from Fig. 9, for the structure with the initial set of parameters.

It can be observed from Fig. 10 that the impedance Z_4 (and thus the impedance Z_{in} from Fig. 9) has the imaginary part equal to zero and the real part equal to $Z^c{}_w$, precisely at the resonant frequencies (ZOR and FP), which implies that the matching condition is fulfilled at these frequencies.

Table 1 gives an overview of the calculated resonance frequencies using the relations (16) and (17), and those obtained using the full-wave simulation, for five different channel lengths.

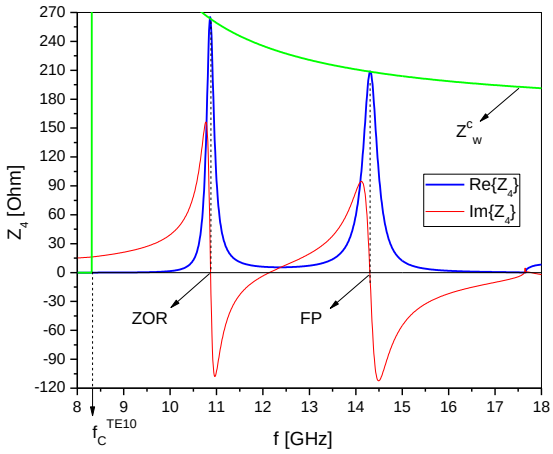

Fig. 10. Real and imaginary parts of the impedance Z_4 from Fig. 9

Table 2 gives an overview of the calculated resonance frequencies using the relations (16) and (17), and those obtained using the full-wave simulation, for five different dielectrics filling the channel.

TABLE 1
COMPARISON OF THE ZOR AND FP RESONANCES OBTAINED USING THE TUNNELING CONDITIONS AND FULL-WAVE SIMULATION FOR VARIOUS CHANNEL LENGTHS, L_{ch} (ε_{rw}=5.95 AND ε_{rch}=3)

	ZOR [GHz] (Equivalent circuit)	ZOR [GHz] (full-wave)	$\lvert\delta_{ZOR}\rvert$ [%]	FP [GHz] (Equivalent circuit)	FP [GHz] (full-wave)	$\lvert\delta_{FP}\rvert$ [%]
L_{ch}=7mm	11.06	11.14	0.72	14.90	14.75	1.02
L_{ch}=9mm	11.12	11.19	0.63	13.76	13.72	0.29
L_{ch}=11mm	11.16	11.22	0.53	13.04	13.04	0
L_{ch}=13mm	11.19	11.24	0.44	12.58	12.61	0.24
L_{ch}=15mm	11.22	11.26	0.36	12.27	12.30	0.24

TABLE 2
COMPARISON OF THE ZOR AND FP RESONANCES OBTAINED USING THE TUNNELING CONDITIONS AND FULL-WAVE SIMULATION FOR VARIOUS DIELECTRICS IN THE CHANNEL (ε_{rw}=5.95)

	ZOR [GHz] (Equivalent circuit)	ZOR [GHz] (full-wave)	$\lvert\delta_{ZOR}\rvert$ [%]	FP [GHz] (Equivalent circuit)	FP [GHz] (full-wave)	$\lvert\delta_{FP}\rvert$ [%]
ε_{rch}=2	13.15	13.35	1.50	16.57	16.17	2.47
ε_{rch}=3	11.06	11.14	0.72	14.90	14.75	1.02
ε_{rch}=4	9.71	9.74	0.31	13.49	13.19	2.27

Table 3 gives an overview of the calculated resonance frequencies using the relations (16) and (17), and those obtained using the full-wave simulation, for five different channel heights.

TABLE 3
COMPARISON OF THE ZOR AND FP RESONANCES OBTAINED USING THE TUNNELING CONDITIONS AND FULL-WAVE SIMULATION FOR VARIOUS CHANNEL HEIGHTS, b_{ch} (ε_{rw}=5.95 AND ε_{rch}=3)

	ZOR [GHz] (Equivalent circuit)	ZOR [GHz] (full-wave)	$\lvert\delta_{ZOR}\rvert$ [%]	FP [GHz] (Equivalent circuit)	FP [GHz] (full-wave)	$\lvert\delta_{FP}\rvert$ [%]
b_{ch}=0.1mm	11.13	11.20	0.63	15.46	15.40	0.39
b_{ch}=0.2mm	11.07	11.14	0.63	15.02	14.92	0.67
b_{ch}=0.254mm	11.06	11.14	0.72	14.90	14.75	1.02
b_{ch}=0.3mm	11.05	11.14	0.81	14.82	14.64	1.23
b_{ch}=0.4mm	11.08	11.15	0.63	14.74	14.46	1.94

It can be seen from Tables 1, 2 and 3 that the maximum error between the calculated and simulated ZOR and FP frequencies are less than 1.5% for the ZOR resonance, and less than 2.5% for the FP resonance, even in the case of pronounced non-homogeneity of the input waveguides, i.e. in the case when the ratio between the relative dielectric permittivities in the input waveguide and the channel is greater than 2, which is a very good agreement. Based on this, one can draw the conclusion that the relations (16) and (17) describe in a very good way the condition that is necessary to fulfill at the resonant frequencies for a non-homogeneous ENZ waveguide.

VI. CONCLUSION

A simple method for modeling ENZ waveguide structures with the accent on the tunneling effect is proposed using the equivalent circuit approach. A condition necessary for the occurrence of resonances in these structures was derived, and it determines the position of ZOR resonance with the error less than 1.5%, and the position of the FP resonance with the error less than 2.5%, when compared with the values obtained by full-wave simulation. The reason for the partial discrepancy of the obtained results is a consequence of modeling the E-step discontinuity between non-homogeneous input waveguide and homogeneous channel using a shunt capacitor. Expression for the shunt capacitane is derived the under assumption that TE_{10} mode exists in such a structure, which is valid if non-homogeneity is not so obvious. This is confirmed by the increase of the error in predicting the resonant frequencies when a greater difference of relative permittivities of the dielectrics (greater non-homogeneity) in the input waveguide is introduced, and by the fact that the relative error in determining the FP resonance is always much higher than in the case of ZOR resonance. This happens because the

capacitance of the shunt capacitor increases rapidly with frequency, which particularly reflects on the FP resonance, which is always at a higher frequency compared to ZOR.

Thus, the change in waveguide height is not adequately modeled in the case of non-homogeneous input ENZ waveguides that were discussed here, and the possibility of modeling this kind of discontinuity by means of other equivalent circuit, especially in the case of pronounced non-homogeneity (large difference in relative dielectric permittivities in the input waveguide, greater thickness of the channel or the existence of a large number of parallel channels connected to the same input waveguide) should be considered. Further efforts in this area should be directed towards this kind of research and towards studying the effects that arise after narrowing the channel, feeding the structure with a coaxial line, and after adding slots on the channel surface.

ACKNOWLEDGEMENT

We would like to thank Prof. Francisco Medina and Dr Raul Rodriguez-Berral for useful discussion through bilateral cooperation between Serbia and Spain PRI- AIBSE-2011-1119.

This work was financed by the Ministry for Education and Science Republic of Serbia through the project TR32024.

REFERENCES

[1] M. G. Silveirinha and N. Engheta, "Tunneling of Electromagnetic Energy Through Subwavelength Channels and Bends Using ε-near-zero materials", *Physical Review Letters*, vol. 97, 157403, 2006.

[2] B. Edwards, A. Alu, M. E. Young, M. G. Silveirinha, N. Engheta, "Experimental verification of epsilon-near-zero metamaterial coupling and energy squeezing using a microwave waveguide", *Physical Review Letters*, vol. 100, 033903, 2008.

[3] R. Liu, Q. Cheng, T. Hand, J. J. Mock, T. J. Cui, S. A. Cummer and D. R. Smith, "Experimental Demonstration of Electrmagnetic Tunneling Through an Epsilon-Near-Zero Metamaterial at Microwave Frequencies", *Physical Review Letters*, vol. 100, 023903, 2008.

[4] L. Liu, C. Hu, Z. Zhao and X. Luo, "Multi-passband Tunneling Effect in Multilayered Epsilon-Near-Zero Metamaterials", Optix Express, vol. 17, pp. 12183-12188, 2009.

[5] M. Mitrović, B. Jokanović, "Field tunneling and losses in narrow waveguide channel", *Microwave Review* 16-2, pp. 8-13, 2010.

[6] M. Mitrović, B. Jokanović and N. Vojnović, "Experimental Verification of Wideband Tuning of the Tunneling Frequency in ENZ Channel", at the Metamaterials' 2012: 6th Int. Congr. Advanced Electromagnetic Materials in Microwaves and Optics, St. Petersburg, Russia, Sept. 2012.D. Powell, A. Alu, B. Edwards, A. Vakil, Y. Kivshar, N. Engheta, "Nonlinear control of tunelling through an epsilon-near-zero channel", *Physical Review Letters*, vol. 79, 245135, 2009.

[7] D. Powell, A. Alu, B. Edwards, A. Vakil, Y. Kivshar, N. Engheta, "Nonlinear control of tunelling through an epsilon-near-zero channel", *Physical Review Letters*, vol. 79, 245135, 2009.

[8] F. Medina, F. Mesa, D. C. Skigin, "Extraordinary transmission through arrays of slits: A circuit theory model", *IEEE Transactions on MTT*, vol. 58, pp. 105-115, 2010.

[9] R. Yang, R. Rodriguez-Berral, F. Medina, Y. Hao, "Analytical model for the transmission of electromagnetic waves through arrays of slits in perfect conductors and lossy metal screens", *Journal of Applied Physics*, vol. 109, 103107, 2011.

[10] L.Zhao, Y. G. Ma, C. K. Ong, "Simulation of Current Experiments on the Tunneling Effect of Narrow ε-Near-Zero Channels", arXiv: 0804.4027v1, 2008.

[11] N. Marcuvitz, *Waveguide Handbook*, New York: McGraw-Hill, 1951.

[12] D. M. Pozar, *Microwave Engineering*, New York: John Wiley & Sons, Inc. , 1998.

[13] A. Alu, M. G. Silveirinha, A. Salandrino, N. Engheta, "Epsilon-near-zero metamaterials and electromagnetic sources: Tailoring the radation pattern", *Physical Review B*, vol. 75, 155410, 2007.